

# **Motion-weighted target volume and dose-volume histogram: a practical approximation of four-dimensional planning and evaluation**

Geoffrey Zhang, PhD<sup>1</sup>, Vladimir Feygelman, PhD<sup>1</sup>, Tzung-Chi Huang, PhD<sup>2</sup>, Craig Stevens, MD,  
5 PhD<sup>1</sup>, Weiqi Li<sup>1</sup>, Thomas Dilling, MD<sup>1</sup>

<sup>1</sup> Division of Radiation Oncology, Moffitt Cancer Center, Tampa, Florida, USA

<sup>2</sup> Department of Medical Radiological Technology, China Medical University, Taiwan

Motion-weighted DVH: an approximation of 4D-planning

10

Corresponding author: Vladimir Feygelman, PhD

Division of Radiation Oncology

Moffitt Cancer Center

12902 Magnolia Drive, Tampa, FL 33612

15 v. 813 745 2757

fax 813 745 7231

[Vladimir.feygelman@moffitt.org](mailto:Vladimir.feygelman@moffitt.org)

**Background and Purpose** In ITV-based 3D-planning, the information of volume occupancy versus respiratory phase is not utilized. We propose a motion-weighted CTV (mwCTV) delineation method, which carries some 4D-information into planning. This method allows plan optimization based on occupancy-weighting and generation of motion-weighted DVH (mwDVH) that approximate the DVHs of full 4D-dose accumulation.

**Material and Methods** Occupancy information from contours in 4D-CT is incorporated in the mwCTV generation. Higher-occupancy volumes receive higher dosimetric priority in planning. The temporally-weighted mwCTV is converted to a spatially-weighted mwCTV incorporating the temporal-weighting in mwDVH generation using the 3D-dose distribution. The mwDVHs were compared with DVHs of deformable-image-registration (DIR)-based 4D-dose accumulation and 3D-method for 10 cases.

**Results** For all the cases, the mwDVH curves are closer to the 4D-calculated DVH than the 3D-DVHs are, indicating a better approximation of the 4D-DVH. The 70Gy-covered percentage-CTV volume differed by  $-2.8\% \pm 0.8\%$  between 3D and 4D, and  $0.3\% \pm 0.7\%$  between mwDVH and 4D-methods. The mean RMS values of the percentage-volume differences for the 4D-3D is  $1.7 \pm 1.1$ , while for the 4D-mwDVH is  $0.4 \pm 0.3$ .

**Conclusion** The mwCTV and mwDVH method, which is simple in implementation and does not require DIR, is a practical approximation of DIR-based 4D-planning and evaluation.

**Key words:** 4D-treatment planning, dose-volume histogram, tumor motion, deformable image registration

## Introduction

45

To potentially improve accuracy of dose delivery, it is considered beneficial to perform four-dimensional (4D) treatment planning incorporating the information contained within the 4D-CT images [1-5]. Many of the proposed techniques require the use of deformable image registration (DIR) to summate doses from the individual respiratory phases. However, this approach is computationally intensive [6] and its reliability can degrade significantly in the presence of imaging artifacts [7].

On the other hand, 4D-CT is widely used in clinical practice to delineate the planning target volume (PTV), which takes the tumor motion into account [8, 9]. Most commonly, the gross target volume (GTV) is contoured on the individual CT phases, and the union of the GTVs on all the phases is called the internal gross target volume (IGTV). The IGTV is further expanded to the internal target volume (ITV) [10, 11] with clinically appropriate margins to cover microscopic disease extension. Finally, the ITV is expanded to create the planning target volume (PTV). Another method to generate a PTV from 4D-CT images is to use the maximum intensity projection (MIP) and margins [1, 12]. These PTV generation techniques can be performed within many commercial software packages. Another target volume generation technique uses mid-ventilation target volume with a proper margin [13, 14]. While fast and practical, these methods of PTV delineation have a major deficiency — they do not fully utilize all the information available in the 4D-CT data set. The expansion from IGTV to ITV to PTV is rooted in legacy three-dimensional (3D) planning techniques based upon static CT data. After the ITV expansion, the temporal information is lost, and the planning process does not differ in principle from traditional static 3D-planning.

65

In this work, we propose a different means to delineate the PTV, which preserves some of the 4D-information throughout the planning process. Weighting information, based on the volume occupancy time of the target throughout the individual respiratory phases, can be used in treatment planning objectives to generate plans with improved dosimetric coverage for mobile targets. Baum *et al* [15] used similar weighting information, generated from daily pre-treatment CT images, in the optimization of intensity modulated radiotherapy to overcome the problem of margin definition in the case of overlapping planning target volume and organs at risk in prostate cancer treatment. In our study, the weighting information is used for a different purpose, to achieve an approximation of 4D-dose DVH without the use of DIR.

As we describe below, this type of approach permits the creation of more realistic motion-weighted dose-volume histograms (mwDVH). Dose mapping based on the use of DIR [4] is not necessary, which makes this method practical in daily clinical treatment planning with commonly-available computing resources.

In this paper, treatment plans were generated for ten lung cancer cases with different tumor sizes and motion ranges. To validate the mwDVH concept, the mwDVH curves for all 10 cases were compared to the DVH curves of the conventional 3D-plans, as well as to curves generated by full 4D-dose mapping and summation based on DIR.

## **Materials and methods**

### **PTV and normal structure generation**

A 4D-CT scan was acquired for each patient for treatment planning using a 16-slice Brilliance Big Bore CT scanner (Philips Medical Systems, Cleveland, OH). The 4D-CT scans incorporated ten separate phases, using a phase binning mode in which the phases were equally spaced in time throughout the respiratory cycle. The 4D-dosimetry research was conducted

90 retrospectively under an institutional review board (IRB)-approved protocol. In our proposed method, the GTV was contoured on each of the respiratory phases in a conventional manner. Next, however, instead of generating the union of all GTVs across the phases (IGTV), we expanded each GTV to a CTV with a margin of 7 mm in all directions on each individual respiratory phase. Figure 1 graphically demonstrates the difference between the proposed method  
95 of contouring and the conventional one. A union of all such CTVs forms the new internal CTV (ICTV) which is the PTV in ITV-based 3D-treatment-planning if the CTV to PTV expansion margin is set to zero. In our proposed method, this ICTV incorporating the weighting information is referred as motion-weighted CTV, or mwCTV. With only two respiratory phases illustrated in Figure 1 for clarity, the mwCTV contains two distinct sub-volumes. The  
100 overlapping part (mwCTV100) is the sub-volume of space that is always occupied by the CTV, while the rest (mwCTV50) is occupied by the CTV 50% or less time during the respiratory cycle. When multiple respiratory phases are used, multiple sub-volumes with different temporal weightings would comprise the mwCTV. In the ten cases, the mwCTV incorporated sub-volumes from all ten phases of the 4D-CT scan. **An in-house program developed in Visual C++  
105 was used for the sub-volume determination using the contours exported from the treatment planning system. This program is easier to use than Pinnacle to generate the sub-volumes but it was validated against Pinnacle.**

The same approach was applied to normal structures to generate motion-weighted organ at risk volumes (mwOAR), but without any margin expansion in individual phases or to the  
110 union. **The lungs were analyzed for all cases and the liver for two of them in which a right lower lobe tumor was in proximity with the right hemidiaphragm. In those latter cases, the entire liver was encompassed within the 4D CT scan. .**

#### 4D-planning and motion-weighted DVH

115           Upon completion of the contouring, we generated treatment plans retrospectively using  
the Pinnacle® planning system (Version 8.0m, Philips Radiation Oncology Systems, Fitchburg,  
WI, USA) for a Trilogy linear accelerator (Varian Medical Systems, Palo Alto, CA, USA). The  
Collapsed Cone Convolution Superposition algorithm [16] was used in dose calculation. The 3D-  
dose distribution was calculated for the ICTV on the **untagged free-breathing** CT image set, from  
120    which the individual phases of the 4D-CT were extracted. This plan was used to generate the  
mwDVH. In the generation of mwDVH, the temporal weightings of the sub-volumes in the  
mwCTV were used as the spatial dose weightings of the volume elements. For example, for a  
volume that is covered by a certain dose 50% of the time, it is considered that 50% of the  
original volume size receives that dose 100% of the time. This weighting concept change makes  
125    it possible to use the 3D-dose distribution from the treatment planning directly for the DVH  
generation without the use of voxel-to-voxel dose mapping for the regions of interest (ROI).

We investigated the accuracy of the approximation when using only two extreme phases  
of the 4D-CT data set, end inspiration and expiration, to generate the mwCTV and mwDVH. We  
generated mwDVH curves using the above-defined methodology, and quantified the differences  
130    between these mwDVH curves and those which incorporated all ten phases of the 4D-scan.

To aid in understanding the weighting concept in treatment planning, we introduced the  
volume ratio:

$$VR_{x\%} = UV_x / UV, \quad (1)$$

where  $UV_x$  is the union volume occupied  $x\%$  of the time in a respiratory cycle,  $UV$  refers to the  
135    total union volume of interest: either the unweighted mwCTV for the target, or mwOAR for the  
organ at risk.

Table 1 demonstrates 10 cases analyzed, with varying tumor sizes and magnitudes of motion, as defined by the centroid displacement between end inhalation and end exhalation.

### **Comparison of mwDVH with 4D-dosimetry using deformable image registration**

140 The optical flow DIR algorithm, which has been validated previously with dose measurements [17], was used for the DIR. We generated deformation matrices from each of the respiratory phases to the base phase (the end-inspiration phase in this study). These matrices were then used to map the dose distributions from all the phases to the base phase, which were then summed with equal weights. With this mapped total dose distribution, DVH curves were  
145 calculated for the CTV and structure volumes defined on the base phase. The mwDVH curves were compared with these 4D-DVH curves based on DIR to assess the validity of our proposed technique. To statistically quantify the differences among the various DVH curves, the root mean square (RMS) values of the percentage-volume differences at fixed doses between the 4D and  
150 3D, 4D and mwDVH curves for all the cases were calculated and compared for the target volumes. A non-parametric Mann-Whitney test was performed on the RMS data to assess the DVH difference/similarity. The non-parametric test was chosen because there is no reason to assume *a priori* that the RMS difference population is distributed normally.

## **Results**

### **155 mwCTV and mwOAR properties**

The center-of-mass motion of the CTV often has an elliptical trajectory. Figure 2 shows an example of an mwCTV generated by incorporating either all ten phases of the 4D-CT scan or only the two extreme phases. The total motion range of the center-of-mass of the CTV was 1.5 cm in this example (Case 2). The ICTV volume was 357.2 cm<sup>3</sup> when all ten phases were

160 included and  $320.2 \text{ cm}^3$  when only the two extreme phases were used. The  $VR_{100\%}$  was 0.414 for  
the ten-phase calculation, and 0.493 for the two extreme phases plan. The other  $VR_{x\%}$  values  
were smaller — between 0.043 and 0.092. Normally, the  $VR_{100\%}$  is significantly larger than the  
ratios for the other weightings. This larger volume of  $VR_{100\%}$  was used in treatment planning  
with high priority in dose coverage. The objective set to this volume was to cover 100% of the  
165 volume by the prescription dose.

Table 1 lists the  $VR_{100\%}$  values as well as the range of motion of the center-of-mass and  
the volume for all 10 cases. All 10 phases were used for calculations in each case. The equivalent  
volume of an mwROI, in which the temporal weightings were considered as spatial weightings,  
is the average of all the volumes of the ROI in all the relevant respiratory phases.

#### 170 **Motion-weighted target DVH compared to 3D-DVH and 4D/DIR DVH**

Motion-weighted DVH curves were generated and compared with the conventional 3D-  
DVHs and the ones generated with 4D-dose calculations using DIR. For Case 10, shown as an  
example in Figure 3, the low dose region in the ICTV was in the low temporal occupancy sub-  
volumes. In the mwDVH calculation for the CTV, the volume of the low dose region was  
175 assigned, as explained above, the same weight as the temporal occupancy weight. Since this  
temporal weight is lower than 1, the mwDVH is more “square” than the ITV-based 3D-DVH.

The CTV mwDVH in Figure 3 was calculated twice: first, using all ten respiratory phases  
(CTV – mw 10ph) and then incorporating only the two extreme ones (CTV – mw 2ph). The  
mwDVH resulting from the two-phase approximation is virtually indistinguishable from the full  
180 ten-phase calculation. Both mwDVH curves are closer to the 4D-calculated DVH (CTV – 4D)  
than the 3D-DVH (ICTV – 3D) is, indicating a better approximation of the 4D-DVH.



Similar results were obtained in all 10 cases analyzed. Figure 4 compares percentage coverage of the target volume by 70 Gy for the 3 different techniques, ITV-based 3D (3D ICTV), mwDVH (mwCTV-10ph, mwCTV-2ph) and 4D using DIR (full 4D). By visual inspection, the values for the mwDVH curves were significantly closer to the ones for the 4D-DVH curves than the 3D-DVH curves were. The values of the average relative difference of the percentage coverage of the target volume by 70 Gy and one standard deviation for the 10 cases between 3D and 4D, mwCTV-10ph and 4D, mwCTV-2ph and 4D are  $-2.8 \pm 0.8\%$ ,  $0.3 \pm 0.7\%$ , and  $0.5 \pm 0.5\%$  respectively, which quantitatively support the above observation. Furthermore, incorporation of only the two extreme respiratory phases for the mwDVH calculations (mwCTV-2ph) demonstrated a reasonable approximation of the full 10-phase calculations (mwCTV-10ph) for all the 10 cases, which is consistent with other studies [18, 19].

The RMS values of the percentage target volume differences at fixed doses over the whole dose range (0 Gy to the maximum dose in the plans) for individual cases are listed in Table 2. The mean RMS values over the 10 cases with one standard deviation for the 4D - 3D difference is  $1.7 \pm 1.7$ , while for the 4D - mwDVH difference is  $0.4 \pm 0.3$  and  $0.4 \pm 0.2$  for 10-phase and 2-phase mwDVH calculations, respectively. This is a clear indication that the mwDVHs for both 10-phase and 2-phase calculations, are a better approximation of the 4D-DVH than the 3D one is. The p values of the Mann-Whitney tests on the RMS data sets of 4D - 3D difference and 4D - mwCTV 10-phase difference were  $\leq 0.0001$ , indicating statistically significant difference between the medians. The p value of the test on the RMS data sets of 4D - mwCTV 10-phase and 4D - mwCTV 2-phase was 0.6, indicating strong similarity between the 10-phase and 2-phase mwCTV DVH curves.

### **Motion-weighted DVH for normal structures**

205 Analogous to the mwCTV generation method described above, the normal structure volume is the union of all the contoured volumes in all the respiratory phases in 3D-planning, but without any margin expansion. The motion-weighted volume of an mwOAR represents the average of all the contoured volumes of the structure. The motion-weighted volume is always smaller than or equal to the volume in 3D-planning, analogous to the mwCTV.

210 The difference between the conventional DVHs and mwDVHs can be more pronounced in normal structures due to increased dose gradients across the normal tissues. Figure 3 demonstrates different DVHs for a right-sided lung cancer case (Case 10). The mwOAR curves indicate higher lung dose compared to the conventional DVH, with the CTV DVHs exhibiting the same trend. The two major reasons behind this effect are the fact that the involved structure  
215 volume is larger with the conventional planning, and that the high dose is mostly concentrated in the 100% occupancy sub-region of the lung. However, the latter is not always the case, as shown for the liver in Figure 3. Although the motion-weighted volumes are smaller than the conventional ones, the high dose is prevalent in the low occupancy sub-regions, so the mwOAR curves are usually lower than the conventional DVHs for liver.

220 The mwDVHs for the right lung and liver when using ten or two respiratory phases are similar to each other for each organ in (Figure 3). This is due to the large relative volumes of these structures, leading to a smaller relative volume difference between the mwOARs derived from ten or two phases. Whether using mwDVHs incorporating only two respiratory phases or all ten, the DVH curves more closely approximate those generated by the 4D-DIR method than  
225 the conventional DVHs, indicating that our methodology more closely approximates 4D-dosimetry than standard methods. The difference between the mwDVH and the DIR-based DVH

for normal structures is larger than for the CTV (Figure 3 is an example). However, mwDVH is still an improvement compared to the standard 3D one.

## Discussion

230           The sub-volumes in the mwCTV should possess different importance in treatment planning. For example, the lost coverage in mwCTV50 should not be as important as the lost coverage in mwCTV100. The lost coverage in mwCTV100 means that 100% of the time a part of the CTV is at a lower than desired dose, while the lost coverage in mwCTV50 means that only 50% of the time a part of the CTV is underdosed. Consequently, the coverage of the mwCTV100  
235           should have a higher dosimetric priority than that of mwCTV50. For example, the prescribed isodose coverage to mwCTV100 could be set at 100% while coverage to the mwCTV50 could be selectively relaxed if it helps to spare the normal structures.

          Normally, the high occupancy volumes are in the center of the ICTV, which are usually covered by higher dose. Loss of dose coverage usually occurs in the peripheral regions of the  
240           ICTV, which in ITV-based 3D-dosimetry are incorrectly assumed to be occupied 100% of the time, while in 4D-dosimetry they are correctly notated as being occupied by tumor a fraction of the time. Thus, as long as the CTV sits within the ICTV, which is true by definition if a setup error is not considered, 4D/DIR CTV DVH curves should be better in dose coverage than that of 3D in most cases. This finding has been observed in this study, and is consistent with research by  
245           Admiraal *et al* [1].

          There are some differences between the ICTV volumes generated using all ten respiratory phases and only the two extreme ones. These differences are caused by missing volume along the motion path, which is often elliptical, due to either only two phases being included, or to contour variations introduced by manually contouring on the other eight phases. The ICTV generated

250 using all ten phases is always larger than the two-phase ICTV. The 100% occupancy volume of the mwCTV is often the same (Figure 2), although the  $VR_{100\%}$  value is always greater for the two-phase mwCTV. There is a concern that the two-phase ICTV may exclude a portion of the ICTV volume due to motion along other axes.

One solution is to use the ICTV generated in a conventional manner from all ten phases  
255 and then use the weighting information from the two-phase mwCTV. In this approach, the conventionally generated ICTV, which has the same volume as the ten-phase ICTV, is divided into two occupancy sub-volumes: 100% occupancy, which is obtained from the two-phase mwCTV, and all other occupancies combined. A total of three sets of contours are needed with this approach.

260 The other solution to reducing the contouring time while maintaining target volume accuracy is to use DIR to automatically generate the additional nine sets of contours from one manually contoured set [6]. All ten sets of contours can then be utilized in treatment planning.

If a robust DIR method is available, then the latter approach is preferable, as the second-level occupancy weighing can be optimized while setting the treatment planning objectives. For  
265 example, the mwCTV  $VR_{100\%}$  is only 0.25 for Case 1 (Table 1). Setting a tight dose coverage objective for this small fractional volume in the mwCTV is less desirable compared to assigning it to a larger volume. In this case, with its large range of motion (1.7 cm), it is more useful to gear the tight dose coverage objective towards the combined lesser occupancy sub-volumes, since in aggregate they account for the majority of the occupancy time ( $CVR_{50\%}=0.71$ ). However  
270 the opposite situation is more frequent. Because the  $VR_{100\%}$ , in most cases is by far the largest among the differential volume ratios (Table 1), it is often reasonable to give precedence to the mwCTV100 in the treatment planning process and assign a combined lower importance to all the

other mwCTV sub-volumes (second-level occupancy weighting), which simplifies the planning process.

275           When only two or three phases are used in the motion-weighted 4D-planning, manual contouring is still quite practical, which makes our method comparatively easy to implement using currently available commercial treatment planning systems. **DIR has been known to fail in the presence of significant image artifacts [7]. The mwDVH method is much less sensitive to image artifacts, which makes it a useful alternative, especially when appreciable artifacts are**  
280 **present.**

          It is theoretically possible that in some cases with small tumor volume and large range of motion, there would be no overlapping volume between the two extreme phases, and thus no 100% CTV occupancy sub-volumes in mwCTVs. For these cases, using only the two extreme phases is no longer justified. Three or more phases are needed to obtain the proper sub-volumes.  
285   The tighter objectives in treatment planning should be given to a sub-volume with the occupancy weighting lower than 100%. However, when such a large tumor displacement is observed, it is expected that some sort of a motion-reducing technique such as abdominal compression [20] or respiratory gating [21] would be applied. In our clinic, we employ an abdominal compression technique during the stereotactic lung treatments, and among approximately 250 cases analyzed  
290   to date, all have had overlapping volume between the two extreme phases.

          If a respiratory gating technique is used, this motion-weighted 4D-planning technique could still be used for the phases that are within the beam-on time. However, the specific phases chosen for beam-on time demonstrate little motion between them, so the dosimetric gains from using our proposed technique would likely be reduced.

295           The generation of the motion-weighted ROIs is straightforward. The difference between  
mwCTV and mwOAR is that no margin is added for OARs while a margin is added to GTV to  
generate CTV in individual phases for mwCTV. For small serial structures with a maximum  
dose constraint, a margin may be needed for the OAR [22].

300           The occupancy weighting concept used in the motion-weighted planning part of this  
study is similar to the coverage probability concept used by Baum *et al* [15]. However there are  
significant differences. While the weighting information was used by Baum *et al* to optimize the  
dose at the target-OAR interface in prostate cancer treatment, it was applied to optimize the dose  
to a moving target in thoracic cancer treatment planning in our project. Furthermore, the concept  
is expanded to generate an approximation of 4D dose DVH in the plan evaluation part of our  
305 study.

          Strictly speaking, our method is not based on the true 4D-dosimetry. The full 4D-  
dosimetry requires DIR to map dose distributions, voxel-to-voxel, from the different respiratory  
phases. Our method is simple and easy to implement because, at its core, it is still a static 3D-  
dose calculation. This simplified 4D-dosimetry concept has been previously used by Glide-Hurst  
310 *et al* [2]. However their approach still relies on DIR. Our method is different because it does not  
rely on DIR for dose accumulation at all. Instead, the 4D-dose accumulation is accomplished by  
converting the temporal weights of the sub-volumes into spatial weights in the DVH calculations.  
The drawback of this approximation is loss of the dose blurring effect. As the ROI moves, the  
hot/cold spot tends to spread, which causes dose blurring in 4D-dosimetry. Our method uses the  
315 3D-dose distribution on the weighted volumes and thus assumes no dose blurring. To incorporate  
such dose blurring, image registration would be necessary. Despite this DVH variance from the

“gold standard” 4D-DIR approach, however, the mwDVH curves still demonstrate significant improvement over standard 3D-dosimetric analysis.

320 The method introduced in this paper only deals with respiratory motion. For most patients, the respiratory motion during treatment is about the same as that derived from the planning 4D-CT [23]. Daily setup variation in treatment needs to be taken care of by other technologies such as image guided radiotherapy (IGRT) and/or additional margins, which is beyond the scope of this paper. Caution is needed when applying this method to patients with irregular respiration, since the patient’s respiration may differ from the pattern when the planning CT is taken, which could  
325 introduce big differences between the planned and delivered doses [24].

## Conclusions

By altering the contouring sequence and introducing the concept of a motion-weighted planning volume, the temporal information contained within the 4D-CT can be incorporated into the treatment planning process. The motion-weighted DVH better approximates the full 4D-  
330 DVH obtained with deformable image registration, compared to the conventional 3D-DVH. The proposed 4D-approximation method requires only minimal modifications to the current treatment planning systems, and does not require deformable image registration. It is less labor intensive, particularly when only two extreme respiratory phases are used, which we demonstrated to be a valid approximation. It can be an alternative to a full 4D-planning and evaluation, especially  
335 when appreciable artifacts are present in CT images.

## References

- [1] Admiraal, MA, Schuring, D, Hurkmans, CW. Dose calculations accounting for breathing motion in stereotactic lung radiotherapy based on 4D-CT and the internal target volume. Radiother Oncol 2008;86:55-60.
- [2] Glide-Hurst, CK, Hugo, GD, Liang, J, Yan, D. A simplified method of four-dimensional dose accumulation using the mean patient density representation. Med Phys 2008;35:5269-5277.
- [3] Guckenberger, M, Wilbert, J, Krieger, T, et al. Four-Dimensional Treatment Planning for Stereotactic Body Radiotherapy. Int J Radiat Oncol Biol Phys 2007;69:276-285.
- [4] Orban de Xivry, J, Janssens, G, Bosmans, G, et al. Tumour delineation and cumulative dose computation in radiotherapy based on deformable registration of respiratory correlated CT images of lung cancer patients. Radiother Oncol 2007;85:232-238.
- [5] Zhang, P, Hugo, GD, Yan, D. Planning Study Comparison of Real-Time Target Tracking and Four-Dimensional Inverse Planning for Managing Patient Respiratory Motion. Int J Radiat Oncol Biol Phys 2008;72:1221-1227.
- [6] Zhang, G, Huang, T-C, Guerrero, T, et al. Use of three-dimensional (3D) optical flow method in mapping 3D anatomic structure and tumor contours across four-dimensional computed tomography data. J Appl Clin Med Phy 2008;9:59-69.
- [7] Wijesooriya, K, Weiss, E, Dill, V, et al. Quantifying the accuracy of automated structure segmentation in 4D CT images using a deformable image registration algorithm. Med Phys 2008;35:1251-1260.
- [8] Rietzel, E, Liu, AK, Doppke, KP, et al. Design of 4D treatment planning target volumes. Int J Radiat Oncol Biol Phys 2006;66:287-295.



- [9] Wolthaus, JWH, Sonke, J-J, van Herk, M, et al. Comparison of Different Strategies to  
360 Use Four-Dimensional Computed Tomography in Treatment Planning for Lung Cancer Patients.  
Int J Radiat Oncol Biol Phys 2008;70:1229-1238.
- [10] Jin, J-Y, Ajlouni, M, Chen, Q, Yin, F-F, Movsas, B. A technique of using gated-CT  
images to determine internal target volume (ITV) for fractionated stereotactic lung radiotherapy.  
Radiother Oncol 2006;78:177-184.
- 365 [11] Shih, HA, Jiang, SB, Aljarrah, KM, Doppke, KP, Choi, NC. Internal target volume  
determined with expansion margins beyond composite gross tumor volume in three-dimensional  
conformal radiotherapy for lung cancer. Int J Radiat Oncol Biol Phys 2004;60:613-622.
- [12] Underberg, RWM, Lagerwaard, FJ, Slotman, BJ, Cuijpers, JP, Senan, S. Use of  
maximum intensity projections (MIP) for target volume generation in 4DCT scans for lung  
370 cancer. Int J Radiat Oncol Biol Phys 2005;63:253-260.
- [13] Mexner, V, Wolthaus, JWH, van Herk, M, Damen, EMF, Sonke, J-J. Effects of  
Respiration-Induced Density Variations on Dose Distributions in Radiotherapy of Lung Cancer.  
Int J Radiat Oncol Biol Phys 2009;74:1266-1275.
- [14] Wolthaus, JWH, Schneider, C, Sonke, J-J, et al. Mid-ventilation CT scan construction  
375 from four-dimensional respiration-correlated CT scans for radiotherapy planning of lung cancer  
patients. Int J Radiat Oncol Biol Phys 2006;65:1560-1571.
- [15] Baum, C, Alber, M, Birkner, M, Nüsslin, F. Robust treatment planning for intensity  
modulated radiotherapy of prostate cancer based on coverage probabilities. Radiother Oncol  
2006;78:27-35.
- 380 [16] Mackie, TR, Scrimger, JW, Battista, JJ. A convolution method of calculating dose for 15-  
MV x rays. Med Phys 1985;12:188-196.

- [17] Zhang, G, Huang, T-C, Forster, K, et al. Dose mapping: validation in 4D dosimetry with measurements and application in radiotherapy follow-up evaluation. *Comp Meth Prog in Biomed* 2008;90:25-37.
- 385 [18] Huang, T-C, Liang, J-A, Dilling, T, Wu, T-H, Zhang, G. Four-dimensional dosimetry validation and study in lung radiotherapy using deformable image registration and Monte Carlo techniques. *Radiation Oncology* 2010;5:45.
- [19] Rosu, M, Balter, JM, Chetty, IJ, et al. How extensive of a 4D dataset is needed to estimate cumulative dose distribution plan evaluation metrics in conformal lung therapy? *Med*  
390 *Phys* 2007;34:233-245.
- [20] Wulf, J, Hädinger, U, Oppitz, U, Olshausen, B, Flentje, M. Stereotactic radiotherapy of extracranial targets: CT-simulation and accuracy of treatment in the stereotactic body frame. *Radiother Oncol* 2000;57:225-236.
- [21] Hara, R, Itami, J, Kondo, T, et al. Stereotactic single high dose irradiation of lung tumors  
395 under respiratory gating. *Radiother Oncol* 2002;63:159-163.
- [22] McKenzie, A, van Herk, M, Mijnheer, B. Margins for geometric uncertainty around organs at risk in radiotherapy. *Radiother Oncol* 2002;62:299-307.
- [23] Rietzel, E, Rosenthal, SJ, Gierga, DP, Willett, CG, Chen, GTY. Moving targets: detection and tracking of internal organ motion for treatment planning and patient set-up. *Radiother Oncol*  
400 2004;73:S68-S72.
- [24] Hugo, G, Vargas, C, Liang, J, Kestin, L, Wong, JW, Yan, D. Changes in the respiratory pattern during radiotherapy for cancer in the lung. *Radiother Oncol* 2006;78:326-331.

**Conflict of Interest Statement:** No conflict of interest for all authors

**Figure captions**

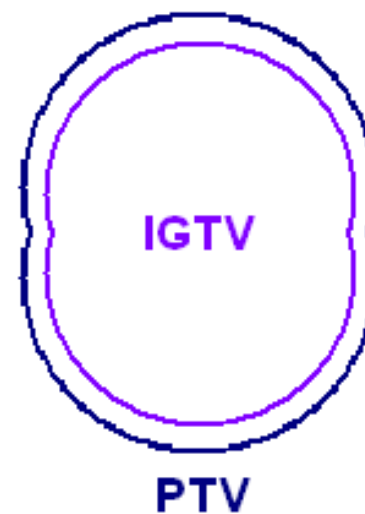
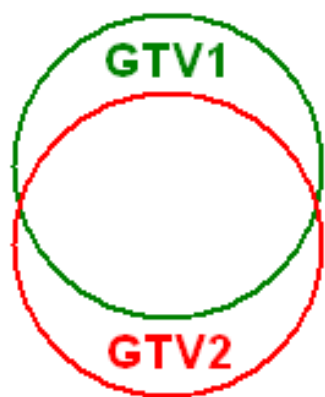
Figure 1 Illustration of the difference between conventional 4D-contouring (top) and the proposed methodology (bottom). Some of the 4D-information is inherent within the motion weighted clinical target volume (mwCTV) while it is absent in the conventional PTV.

Figure 2 Motion-weighted clinical target volume (mwCTV) incorporating different numbers of respiratory phases for Case 2. The mwCTV100, is often the same if all ten or only two extreme phases are used. The occupancy weighting, defined as the time fraction of CTV occupancy in a respiratory cycle in mwCTV, is scaled from black as 0% to red as 100%.

Figure 3 A comparison between mwDVH, conventional DVH and 4D-calculated DVH of target volume, right lung and liver for Case 10. Both mwDVH curves, using either 10 phases in the 4D-CT set (denoted as 10 ph) or only the 2 extreme phases (denoted as 2 ph) are a better approximation of the 4D-calculated DVH (denoted as 4D) than the DVH calculated using a 3D-technique (denoted as 3D) is.

Figure 4 A comparison of the percentage target volume covered by a dose of at least 70 Gy for DVH curves generated using 3D, motion-weighted and 4D-methods respectively, for all the 10 cases studied. Two-phase approximation for the motion-weighted method, in which only the two extreme phases were used for mwDVH calculations, is also included in this comparison.

conventional method



proposed method

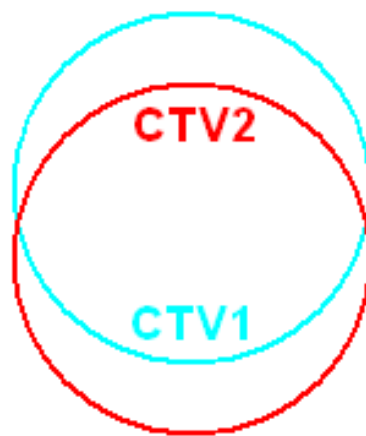
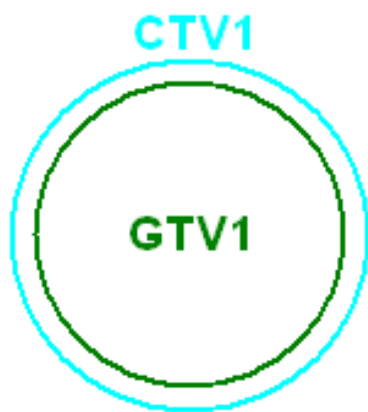
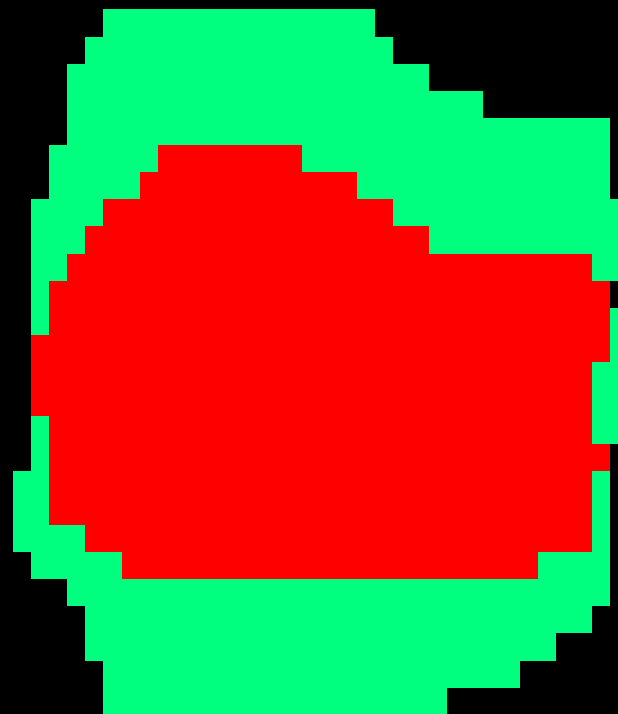
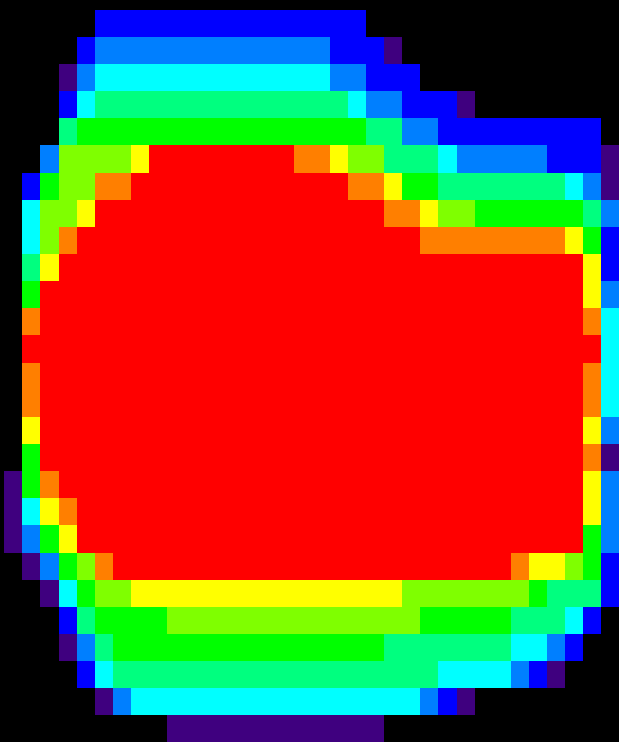


Figure 1

**10-phase**

**2-phase**



**0**

**50%**

**100%**

Figure 2

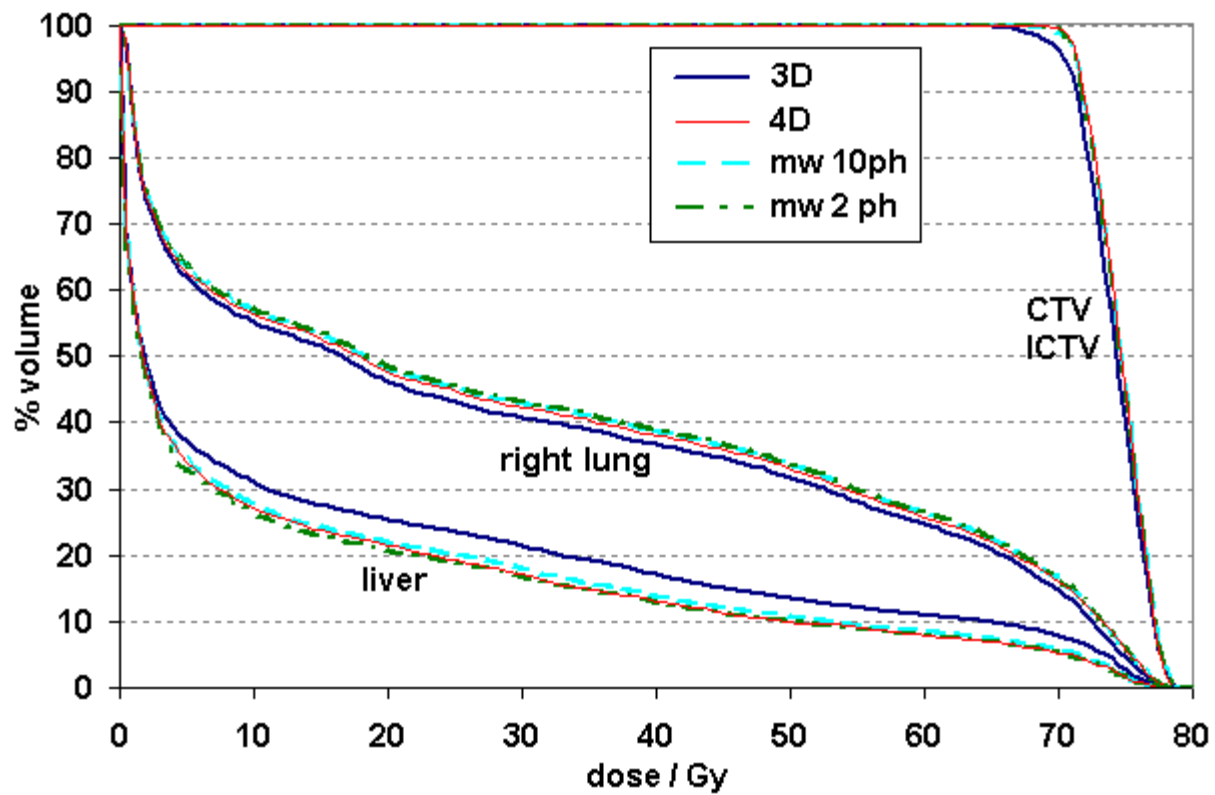


Figure 3

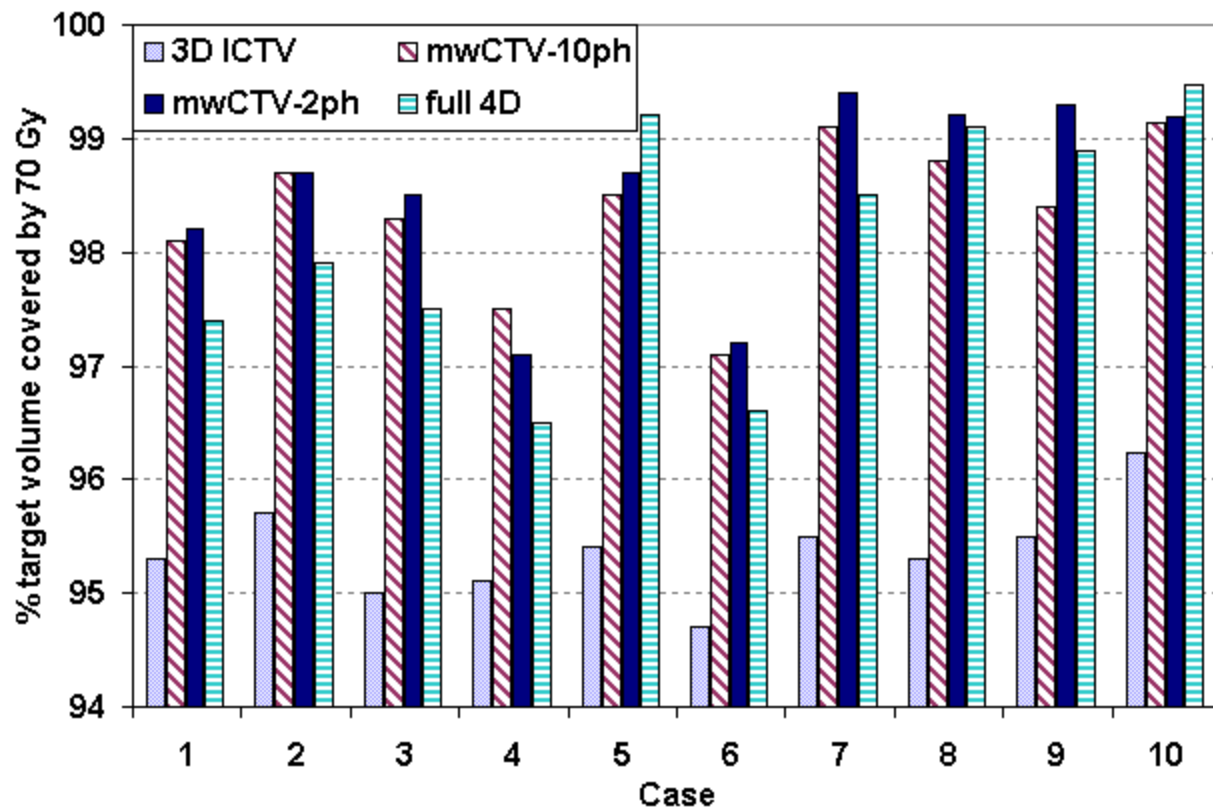


Figure 4